Volcanic winter and accelerated glaciation following the Toba super-eruption

Michael R. Rampino*† & Stephen Self‡

* Earth Systems Group, Applied Science Department, New York University, New York, New York 10003, USA
† NASA, Goddard Institute for Space Studies, New York, New York 10025, USA
‡ Department of Geology and Geophysics, School of Ocean and Earth Science and Technology, University of Hawaii at Manoa, Honolulu, Hawaii 96822, USA

THE eruption of Toba in Sumatra 73,500 years ago was the largest known explosive volcanic event in the late Quaternary[1]. It could have lofted about 10^{15} g each of fine ash and sulphur gases to heights of 27–37 km, creating dense stratospheric dust and aerosol clouds. Here we present model calculations that investigate the possible climatic effects of the volcanic cloud. The increase in atmospheric opacity might have produced a 'volcanic winter'[2]—a brief, pronounced regional and perhaps hemispheric cooling caused by the volcanic dust—followed by a few years with maximum estimated annual hemispheric surface-temperature decreases of 3–5 °C. The eruption occurred during the stage 5a-4 transition of the oxygen isotope record, a time of rapid ice growth and falling sea level[3]. We suggest that the Toba eruption may have greatly accelerated the shift to glacial conditions that was already underway, by inducing perennial snow cover and increased sea-ice extent at sensitive northern latitudes. As the onset of climate change may have helped to trigger the eruption itself[4], we propose that the Toba event may exemplify a more general climate–volcano feedback mechanism.

The Toba pyroclastic deposits on Sumatra near to the source (equal to 2,000 km^3 of magma) have been radiometrically dated at 73.5 ± 3.5 kyr and 73 ± 4 kyr before present (ref. 1). The widespread Toba ash layer (800 km^3 of magma)[1] occurs in Indian Ocean deep-sea cores within the oxygen isotope stage 5a-4 transition[3]. The duration of eruption has been estimated as up to two weeks[5], and the eruptive flux as $\sim 7 \times 10^9$ kg s^{-1}, implying eruption cloud heights from 27 to 37 km (ref. 6).

Petrological studies suggest that $\sim 3 \times 10^{15}$ g of H_2S and SO_2 (convertible to $\sim 1 \times 10^{16}$ g of H_2SO_4 aerosols) could have been released from the erupted magma[1]. Although the intrinsic sulphur content of silicic magmas is low[2], efficient degassing and the large volume of magma erupted combine to give an enormous volatile release. Extrapolation from smaller historical eruptions[2] suggests a lower amount of aerosol (1.5×10^{15} g) for Toba, along with $\sim 2 \times 10^{16}$ g of fine (<2 μm) dust. Condensation and coagulation in aerosol clouds may considerably reduce the amount of long-lived H_2SO_4 aerosols[7]. At present, however, there are no data on the behaviour of H_2SO_4 aerosols in such dense clouds.

The amount of stratospheric water available to convert SO_2 to H_2SO_4 may limit aerosol loading. At present, $\sim 4 \times 10^{15}$ g of ambient water[8] might be available in the form of H_2O and CH_4. Toba may have released as much as 5.4×10^{17} g of H_2O (ref. 1), so enough could have been present in the stratosphere to convert the sulphur gases emitted by Toba into $\sim 1 \times 10^{16}$ g of H_2SO_4 aerosols. To be conservative, however, and in agreement with extrapolations from historic eruptions, we assume that only 10% of this amount of aerosols actually formed in the Toba cloud, or $\sim 1 \times 10^{15}$ g of H_2SO_4 aerosols.

The 1815 Tambora eruption (with an estimated 2×10^{14} g of stratospheric aerosols) may be related to an observed surface temperature decrease of ~0.7 °C in the Northern Hemisphere in the year following the eruption[2]. A linear relationship between hemispheric cooling and aerosol loading would predict cooling by ~3.5 °C in the year following the eruption from an aerosol loading of 1×10^{15} g. Other empirical methods[9] give estimates in the range of 3 to 5 °C.

A stratospheric aerosol burden for Toba of 1×10^{15} g yields a global aerosol optical depth (τ) of about 10 (ref. 2). (Optical depth $\tau = -\ln(I/I_0)$; where I_0 and I are the initial and final light intensity, respectively. For volcanic aerosols and dust, τ is largely dependent on the single scattering albedo (ω) of the cloud, whereas for soot (smoke) clouds, the absorption optical depth τ_a is primarily a function of the high absorptivity of the soot particles in the visible (fluffy soot also absorbs in the infrared).) A stratospheric injection of 10% of the estimated fine dust generated would produce a dust-cloud optical depth of ~10 for a few months. The low-latitude position of Toba would probably have led to efficient injection of dust and volatiles into the stratosphere in both hemispheres[2]. The estimated optical depth increase from the dust and aerosols is equivalent in visible opacity to smoke-cloud absorption optical depths of ~2 to 3, used in nuclear-winter scenarios for a full-scale nuclear war[10–12].

In simulations of the first 1 to 3 months of a nuclear winter (for a worst-case July smoke injection) global climate models

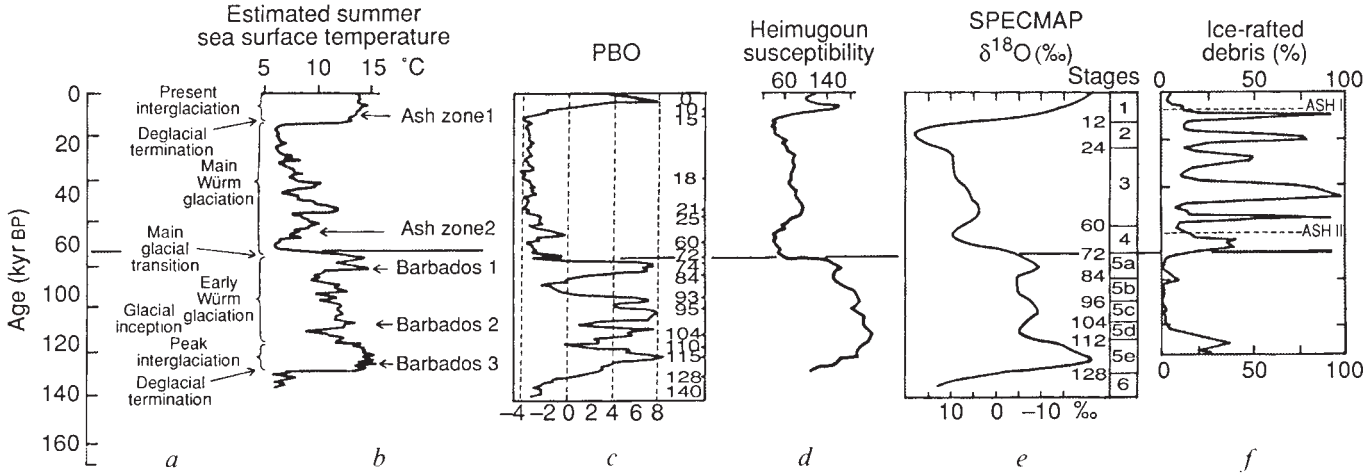

FIG. 1 Climate indicators for the past 140 kyr. *a*, Climatic states[33]. *b*, Reconstructed summer SST (planktonic foraminiferal assemblage data), deep-sea core V23-82, North Atlantic[15]. Dates: Ash Zone 1 (9.5 kyr), Ash Zone 2 (65 kyr), Barbados 1 Terrace (~85 kyr), Barbados 2 (~110 kyr) and Barbados 3 (~125 kyr). *c*, Palaeobioclimatic operator (PBO), a measure of the 'best possible' climate profile based on multivariate statistical analysis of Les Echets, France pollen records. Higher PBO indicates warmer climate. The vertical scale is nonlinear[45]. *d*, Magnetic susceptibility, Heimuguon loess section, Central China. Loess in palaeosols formed in warm intervals has higher susceptibility than loess deposited in cold intervals[46]. *e*, SPECMAP $\delta^{18}O$ scale. Stages and dates of boundaries shown at right[3]. $\delta^{18}O = [(^{18}O/^{16}O)_{sample}/(^{18}O/^{16}O)_{standard}] - 1$, where standard is PDB (cretaceous belemnite carbonate). *f*, Percentage of ice-rafted detritus in North Atlantic deep-sea core Me69-17. Depth in metres[14].

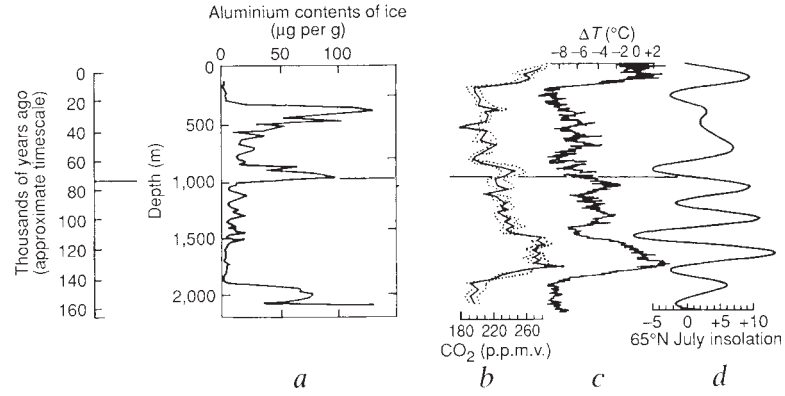

FIG. 2 Vostok ice-core climate records[21], and climatic forcings for the past 160 kyr. For ice-core data, timescale is approximate. *a*, Aluminum content of ice, indicating continental wind-blown dust. Vertical scale is in metres depth. *b*, Atmospheric CO_2 from trapped air bubbles. *c*, Temperature deviations (°C) from present, based on δD measurements. *d*, July insolation at 65° N (per cent deviation from present)[48].

(GCMs) predict that land temperatures in the latitude zone 30° to 70° N could range from ~5 to ~15 °C colder than normal, with widespread immediate hard freezes in mid-latitudes, and possibly considerable precipitation decreases[10]. At lower latitudes, GCM simulations suggest immediate coolings of ~10 °C (ref. 11). During the first 1 to 3 years, global average τ_a of 0.5 could persist, with cooling of 5 °C in areas covered by the smoke cloud. Ocean-surface cooling of ~2 to 6 °C may extend for several years[10]. The persistence of significant soot optical depths for 1-3 years might lead to longer-term (decadal) cooling, primarily through increased snow cover and sea ice, and perturbed sea surface temperatures[10-11].

The injection of massive amounts of volcanic dust into the stratosphere by a super-eruption such as Toba, with aerosol optical depths of ~10, might be expected to cause similar immediate surface cooling, creating a 'volcanic winter'[2]. Volcanic dust has a shorter residence time in the atmosphere (3-6 months) than soot[10,11], and hence the effects might be more limited in area and in time. But the coincident injection of $\sim 10^{15}$ g of sulphur volatiles into the stratosphere, and the time required for the formation and spread of the resulting H_2SO_4 aerosols, should extend the period of increased atmospheric opacity and surface cooling. A maximum e-folding residence time for the aerosols in the stratosphere of about a year[2] (ignoring possibly important self-limiting mechanisms) would lead to several years with optical depths ≥ 0.1.

The Toba eruption occurred during a major Late Quaternary climate event, the $\delta^{18}O$ stage 5a-4 boundary, which is the interval of most rapid ice accumulation, and the main Northern Hemisphere warm-cold transition of the last glacial cycle[3,13] (Figs 1 and 2). The transition is marked by a drop in sea level of ~40 m in less than 7,000 years, the first significant peak in ice-rafted detritus in the North Atlantic during the last glacial cycle[14], and a decrease in seasonal sea surface temperatures in the North Atlantic[15] by 10 °C in <5,000 years. Other climate indicators also suggest that the glacial cooling began very abruptly[16-18] at ~74 kyr; changes in ocean bottom-water circulation in the Atlantic may have involved a shut-down of North Atlantic Deep Water formation[19,20], briefly in operation during substage 5a.

At ~74 kyr, Milankovitch parameters were such as to favour the growth of Northern Hemisphere ice sheets, with low summer insolation at high northern latitudes (Fig. 2). Average atmospheric p_{CO_2} decreased from ~245 p.p.m. to ~195 p.p.m. mostly during the final phase of the cooling ~71 to 62 kyr (ref. 21). Atmospheric methane shows a decrease from about 600 to 400 parts per 10^9 (p.p.b.) which is only a minor climate forcing[22]. Increased atmospheric dust content during glacial stages[23] has been suggested to cause global cooling of up to 2-3 °C: the Vostok ice core shows a dust peak at ~71 kyr (Fig. 2). An increase in non-sea-salt sulphur in the Vostok core[24] at the stage 5a-4 boundary suggests a possible minor cooling from increased cloud cover of ~0.6 °C.

Much of the large increase in ice volume occurred next to a warm subpolar ocean[15]. By stage 4, ice volume reached more than 60% of the full glacial maximum of stage 2, with snow and ice fields southward in eastern Canada to ~50 °N (ref. 16). These conditions could be interpreted as supporting the concept of rapid 'glacierization'[25,26], in which summer cooling leads to permanent snowfields and resulting snow-albedo feedback.

A period during which mean daily summer temperatures were lower than present over the central plateau of Quebec and Labrador, perhaps accompanied by increased snowfall, might favour the formation of perennial snow cover[25-28]. Tree-ring data from Northern Quebec show mean summer temperatures for the past 250 years of 9.5 °C, with a lowering of 3.5 °C (to ~6 °C) in 1816 after the Tambora eruption[29]. Northern Hemisphere temperatures decreased by ~0.7 °C in the year after Tambora[2], so that the summer temperature decline in Quebec in 1816 shows roughly a fivefold amplification of hemispheric cooling (although this extreme cooling could be partly a dynamic effect of regional blocking and meridional circulation[30]). If these same factors were important at 74 kyr, then a 3 °C Northern Hemisphere cooling after Toba might have led to Quebec summer temperatures 10-15 °C colder than at present for 2 or 3 years.

Lowering of the freezing line should have a direct effect on annual snow accumulation. July temperatures on the east shore of Hudson Bay at present average 14.2 °C, and the freezing altitude (0° isotherm) averages ~2,500 m (ref. 31). An aerosol cloud like that of Toba might cause the atmospheric freezing altitude to descend to ground level under present July climate conditions, an even more likely occurrence under conditions of increased snow and ice cover and sea-ice extent.

According to the Goddard Institute for Space Studies (GISS) GCM, volcanic aerosols that caused an optical-depth perturbation of 0.1 for 5 years led to a global surface cooling of ~0.5 °C, with a reduction in summer temperatures in Canada at ~55° N of ~2 °C, or 4 times the global average (D. Rind, personal communication). If high-latitude seasonal amplification is roughly linear with temperature decrease, then a 3 °C global cooling after the Toba eruption could have led to a 12 °C reduction in summer temperatures for perhaps ~2 to 3 years in the areas of growth of the Laurentide ice sheet, in good agreement with empirical estimates.

Results of two-dimensional climate models coupled with ice-sheet models[32,33] are in agreement with the inferred isotopic and sea-level changes at the 5a-4 boundary[34], but these models are highly parameterized, and do not rule out a contribution from volcano-induced cooling. By contrast, GCM experiments give mixed results[27,35,36]. Some GCM runs using versions of the NCAR Community Climate Model suggest that imposition of snow cover in the Northern Hemisphere under present conditions can lead to retention and increase in snow depth in glaciation-sensitive areas[35]. Experiments using the GISS GCM[36], however, were unable to initiate the growth of Northern Hemisphere ice sheets even with summer insolation fields lower than that of 74 kyr. The effects of considerable pre-existing land ice

and sea ice on further ice accumulation are not well determined, and the mixed GCM results suggest differences in model sensitivity to factors involved in ice accumulation. Until these are better understood, no firm conclusions should be drawn about ice-growth conditions.

The detailed record of climate and $\delta^{18}O$ during the stage 5a-4 transition reveals that although sea-level lowering[3] began before the Toba eruption, North Atlantic surface-ocean temperatures remained warm[37], and ice-sheet growth was beginning to slow[3]. It may be significant, therefore, that the Toba eruption apparently coincided with a precipitous decrease in North Atlantic surface temperatures and global sea level[3,34]. Increased sea ice and snow cover following the eruption may have provided the extra 'kick' that caused the climate system to switch from warm to cold states[38,39]. Other very large Quaternary eruptions during warm–cold transitions show a similar timing[40,41], and there is also some evidence of increased volcanism during cold–warm transitions[41]. The connection may come through the effects of water loading and unloading on magma chambers during sea-level fluctuations[4], which may explain the apparent relationship between volcanic activity and Milankovitch parameters: Late Quaternary ash layers in deep-sea cores from the Mediterranean[42] and the Indian Ocean[43] have a periodicity of ~23 kyr similar to the Earth's precessional period, and Icelandic[44] and Japanese eruptions (K. Caldeira, personal communication) apparently follow a 100-kyr cycle.

Although correlations have often been claimed between Quaternary climate change and volcanism[4], it was thought that because of the short-lived nature of volcanic aerosols, and the control of the timing of climatic change by Milankovitch cycles, such correlations were unrelated coincidence. Our results may provide a physical explanation: if climatic change can trigger eruptions[4], then short-term volcanic winters caused by dust and aerosols from large eruptions such as Toba might provide positive feedback for cooling at critical times during warm–cold transitions. Volcanic aerosols may also constitute a negative feedback during glacial terminations, contributing perhaps to brief episodes of cooling and glacial readvance such as the Younger Dryas Interval[41]. □

Received 10 December 1991; accepted 9 July 1991.

1. Chesner, C. A. *et al. Geology* **19,** 200–203 (1991).
2. Rampino, M. R., Self, S. & Stothers, R. B. *A. Rev. Earth planet. Sci.* **16**, 73–99 (1988).
3. Martinson, D. G. *et al. Quat. Res.* **7**, 1–29 (1987).
4. Rampino, M. R., Self, S. & Fairbridge, R. W. *Science* **206,** 826–828 (1979).
5. Ledbetter, M. T. & Sparks, R. S. J. *Geology* **7,** 240–244 (1979).
6. Woods, A. W. & Wohletz, K. H. *Nature* **350,** 225–227 (1991).
7. Pinto, J. P., Turco, R. P. & Toon, O. B. *J. geophys. Res.* **94,** 11165–11174 (1989).
8. Stothers, R. B., Wolff, J. A., Self, S. & Rampino, M. R. *Geophys. Res. Lett.* **13,** 725–728 (1986).
9. Palais, J. M. & Sigurdsson, H. *Am. geophys. Un. geophys. Monogr.* **52,** 31–52 (1989).
10. Turco, R. P., Toon, O. B., Ackerman, T. P., Pollack, J. B. & Sagan, C. *Science* **247,** 166–170 (1990).
11. Covey, C., Schneider, S. H. & Thompson, S. *Nature* **308,** 21–25 (1984).
12. National Research Council *The Effects on the Atmosphere of a Major Nuclear Exchange* (National Academy of Sciences, Washington DC, 1985).
13. Ruddiman, W. F. & McIntyre, A. *Science* **204,** 173–175 (1979).
14. Heinrich, H. *Quat. Res.* **29,** 142–152 (1988).
15. Sancetta, C., Imbrie, J., Kipp, N. G., McIntyre, A. & Ruddiman, W. F. *Quat. Res.* **2,** 363–367 (1972).
16. Koerner, R. M. & Fisher, D. A. in *Late Quaternary Environments: Eastern Canadian Arctic, Baffin Bay and West Greenland* (ed. Andrews, J. T.) 309–327 (Allen and Unwin, London, 1985).
17. Woillard, G. & Mook, W. G. *Science* **215,** 159–161 (1982).
18. Guiot, J. *Palaeogeogr. Palaeoclimatol. Palaeoecol.* **80,** 49–69 (1990).
19. Streeter, S. S. & Shackleton, N. J. *Science* **203,** 168–171 (1979).
20. Jouzel, J. *et al. Nature* **329,** 403–407 (1987).
21. Barnola, J. M. *et al. Nature* **329,** 408–414 (1987).
22. DeAngelis, M., Barkov, N. I. & Petrov, V. N. *Nature* **325,** 318–321 (1987).
23. Harvey, L. D. D. *Nature* **334,** 333–335 (1988).
24. Legrand, M. R., Delmas, R. J. & Charlson, R. J. *Nature* **334,** 418–420 (1988).
25. Loewe, F. *Arct. Alp. Res.* **3,** 331–344 (1971).
26. Andrews, J. T. & Barry, R. G. *A. Rev. Earth planet. Sci.* **6,** 205–228 (1978).
27. Williams, J. *J. appl. Meteorol.* **14,** 137–152 (1975).
28. Koerner, R. M. *Quat. Res.* **13,** 153–159 (1980).
29. Jacoby, G. C., Ivanciu, I. S. & Ulan, L. D. *Palaeogeogr. Palaeoclimatol. Palaeoecol.* **64,** 69–78 (1988).
30. Schneider, S. H. *Clim. Change* **5,** 111–113 (1983).
31. Wilson, C. *Syllogeus* **55,** 147–190 (1985).
32. Fichefet, T. *et al. Phil. Trans. R. Soc. Lond.* A**39,** 249–261 (1989).
33. Deblonde, G. & Peltier, W. R. *Clim. Dynam.* **5,** 103–110 (1990).
34. Chappell, J. & Shackleton, N. J. *Nature* **324,** 137–140 (1986).
35. Oglesby, R. J. *Clim. Dynam.* **4,** 219–235 (1990).
36. Rind, D., Peteet, D. & Kukla, G. *J. geophys. Res.* **94,** 12851–12871 (1989).
37. Ruddiman, W. F., McIntyre, A., Niebler-Hunt, V. & Durazzi, J. T. *Quat. Res.* **13,** 33–64 (1980).
38. Matteucci, G. *Clim. Dynam.* **6,** 67–81 (1991).
39. Miller, G. H. & Kaufman, D. S. *Norsk Geol. Tidssk.* **71,** 149–151 (1991).
40. Ruddiman, W. F. & McIntyre, A. *Geol. Soc. Am. Bull.* **93,** 1273–1279 (1982).
41. Dawson, A. *Ice Age Earth: Late Quaternary Geology and Climate,* 180–198 (Routledge, London, 1991).
42. Paterne, M. *et al. Earth planet. Sci. Lett.* **98,** 166–174 (1990).
43. Paterne, M. *et al. IAVCEI Progr. Abstr., Gen. Assembly, Vienna, IUGG* **20,** 6 (1991).
44. Sioholm, J., Sejrup, H. P. & Furnes, H. *J. Quat. Sci.* **6,** 159–173 (1991).
45. Guiot, J. *et al. Nature* **338,** 309–313 (1989).
46. Heller, F., Xiuming, L., Tungsheng, L. & Tongchun, X. *Earth planet. Sci. Lett.* **103,** 301–310 (1991).
47. Ninkovich, D. *et al. Nature* **276,** 574–577 (1978).
48. Berger, A. *Quat. Res.* **9,** 139–167 (1978).

ACKNOWLEDGEMENTS. We thank K. Caldeira, C. Fletcher, D. Peteet, W. F. Ruddiman, S. H. Schneider, R. B. Stothers and G. P. L. Walker for reviews, and D. Rind, W. I. Rose, H. Sigurdsson and A. W. Woods for discussions. This work was supported in part by grants from the U.S. DOE, National Institutes for Global Environmental Change, NASA, the Center for Global Habitability at Columbia University (M.R.) and NATO (S.S.).

Evidence for melt segregation towards fractures in the Horoman mantle peridotite complex

Natsuko Takahashi

Geological Institute, Faculty of Science, University of Tokyo, Tokyo 113, Japan

MELT segregation from a solid matrix in the upper mantle is the first step in the formation of magmas. The mechanisms of melt segregation proposed so far have been based on two different physical models: the percolation of interstitial melt driven by a density difference between melt and matrix, associated with compaction and deformation of the matrix[1]; or the suction of interstitial melt into fractures from a surrounding porous matrix[2–4]. Although the latter process was originally invoked to explain the occurrence of dunite and pyroxenite–gabbro dykes with zones depleted in melt component on both sides[2,5–7], most of these zones are discordant, small in scale and clearly formed by reaction between peridotite and basaltic melt[8]. I have suggested[9] that thick, concordant dunite zones in the most depleted peridotite layers of the Horoman peridotite complex formed by suction of partial melt towards fractures later filled by dunite. Here I report a detailed mineralogical variation across the dunite which, when set in its geological and petrographic context, provides clearer evidence for melt segregation by dynamic forcing[3], rather than passive percolation. This mechanism of melt segregation may play an important role in the formation of primary magmas with low production rate and large geochemical variability.

The Horoman peridotite complex[9–14] in Hokkaido, northern Japan, lies at the southern end of the Hidaka metamorphic belt[15]. The complex is stratified and has a total thickness of ~3,000 m (refs 11, 12). It is composed of the Main Harzburgite-Lherzolite suite (MHL), with a subordinate spinel-rich dunite-wehrlite suite (SDW) and a minor banded dunite-harzburgite suite (Fig. 1)[9,14].

The MHL is composed of harzburgite and lherzolite, which are grouped into harzburgite, symplectite-free spinel lherzolite, symplectite-bearing spinel lherzolite and plagioclase lherzolite on the basis of mineral content and presence or absence of symplectites consisting of intergrowths of ortho- and clinopyroxene plus spinel ('two-pyroxene/spinel' symplectites). These four rock types show gradational changes in modal composition and bulk and mineral chemistries: the modal content of clinopyroxene and orthopyroxene, and the bulk content of CaO and Al_2O_3 decrease, whereas the forsterite content of olivine (Fo) and the Cr/(Cr+Al) atomic ratio (Cr#) of spinel increase from plagioclase lherzolite to harzburgite through symplectite-bearing and symplectite-free spinel lherzolite[9,14]. The variations are cyclic in the field, giving rise to the stratified structure of the Horoman complex. The wavelength of each cycle ranges from several meters to a few hundred metres. The